J Nanopart Res
DOI 10.1007/s11051-010-9953-y

RESEARCH PAPER

Thermal stability and morphological variation of carbon nanorings of different radii during the temperature elevating process: a molecular dynamics simulation study

Chuan Chen · Jee-Gong Chang · Shin-Pon Ju · Chi-Chuan Hwang

Received: 15 September 2009 / Accepted: 27 April 2010
© Springer Science+Business Media B.V. 2010

Abstract We study the thermal stability and morphological variations of nanorings with different radii during the temperature elevation using the molecular dynamics (MD) simulation method. Five metastable nanorings were generated using the different initial C–C bond length of armchair carbon nanotubes. The stable structures of the two smallest nanorings have several kinked regions around the nanorings, with the deformations of the inner and outer walls occurring at the same temperature. For the largest three cases, the morphologies of nanorings from the top view display circular shapes at 0 K. For the nanoring with a radius of 146 Å(350 units), the thermal deformation process is very similar to the smallest two cases, but the temperature at which the thermal deformation begins is higher. For the nanoring with nanoring radii of 165 Å (400 units) and 185 Å (450 units), thermal deformation will take place at the inner wall of the nanoring, and then will induce deformation of the outer wall at a higher temperature. Variations of local structures at the kinked regions at different temperatures are also drawn.

Keywords Carbon nanoring · Morphological variation · Thermal stability · Nanoring · Molecular dynamics simulation · Numerical simulation

C. Chen · C.-C. Hwang (✉)
Department of Engineering Science, National Cheng Kung University, Tainan 701, Taiwan, ROC
e-mail: chchwang@mail.ncku.edu.tw

C. Chen
Department of Information Management, Meiho Institute of Technology, Pingtung 912, Taiwan, ROC

J.-G. Chang
National Center for High-Performance Computing, No. 28, Nan-Ke 3rd Rd, Tainan 744, Taiwan, ROC

S.-P. Ju
Department of Mechanical and Electro-Mechanical Engineering, Center for Nanoscience and Nanotechnology, National Sun-Yat-Sen University, Kaohsiung 804, Taiwan, ROC

Introduction

A carbon nanoring quasi-zero dimensional structure which could conceptually be formed by knitting together the two ends of a carbon nano-tube (CNT) was discovered by Liu et al. (1997). Because CNTs possess many promising mechanical and electronic properties, the CNT as well as carbon nanorings can be used in both electronic (Oh et al. 2000) and mechanical devices (Chen et al. 2005) in an electronic-mechanical system. In these electronic-mechanical systems, thermal effects might be an important factor which influences the structure stiffness (Zhu and Wang 2007) and structure stability (Hod and Rabani 2003; Pozrikidis 2008; Liu et al. 2005). Most importantly, the induced thermal deformation (or structure) will influence the electronic properties (Liu et al. 2001).

Published online: 15 May 2010

Thus, understanding of thermal stability is very important before nanoring or other structures (Berber et al. 2003) can provide building blocks for larger systems. Furthermore, it is helpful to optimize the electronic-mechanical properties to meet the thermal or mechanical conditions as such a system is put into operation.

There is substantial existing literature investigating nanoring physical properties, such as electronic structure (Lin and Chuu 1998a, b; Latge et al. 2003; Shyu et al. 2004), magnetic properties (Lin and Chuu 1998a, b; Liu et al. 2002; Latil et al. 2003; Tsai et al. 2004), optical properties (Lin 1998a, b, c), and transport properties (Shea et al. 2000). Most of these studies use a static approach and do not take the thermal effect into account. Though this research indeed provides valuable information, the important influence of deformation which arises either from the thermal or mechanical loading has for the most part been lacking. In Liu et al.'s (1997) study, they clearly pointed out that there is a dramatic change in the electronic conductance by delocalized deformation. Furthermore, Kwon et al. (2004) found the contraction deformation of the CNT could take place at room temperature and become severe at higher temperature. This conclusion also suggests that thermal deformation needs to be considered to more accurately approach a realistic application.

In more related research, Hod and Rabani (2003) investigated the structure and stability of closed-ring CNTs based on the Tersoff–Brenner potential (Brenner 1990a, b). These metastable structures are produced by geometric folding and relaxed into minimum energy using a minimizing algorithm. They found that short tubes do not stay closed and yet tubes of longer than 18 nm are kinetically stable. The initial structures are suggested by Dunlap (1992), which use the minimization energy method to decide the possible structure. Oh et al. (2000) found that different structures, like D_{5d} and D_{6h} nanotube tori, behave like semiconductors and metal, respectively. Both of these studies have provided deep insight into the stability and electronic properties of nanoring structures; however, dynamic behavior under the temperature environment is not discussed.

Chen et al. (2005) investigated the mechanical properties of the connected carbon nanoring by molecular dynamics (MD) simulation. They found the nanorings are stable under large tensile deformation. The focus of this study is on mechanical strength, thus, the initial configuration of the nanoring is obtained under a certain temperature, but the thermal stability is left unexplored. Huhtala et al. (2002a, b) investigated the defect formation of the nano-toroidal structure obtained by bending the CNT at both low and at very high temperature. They found bond breakages in the pentagon–heptagon pair and that the thermally excited defects seem to settle mainly in the unbuckled regions at high temperature. Similarly, the bond breakage behavior is only found at a specific temperature, and the thermal stability is left unexplored.

The objective of this paper is to investigate the thermal stability and morphological variations of the carbon nanorings of different radii when subjected to a gradual temperature rise. The MD method with the second-generation reactive empirical bond order (REBO II) potential (Brenner et al. 2002) is used to simulate the interaction between carbon atoms. In addition, the Nosè–Hoover thermostat algorithm (Hoover 1985) is used to model a temperature rise procedure. In this paper, we investigate the deformation mechanisms of nanorings of five sizes at differing temperatures, and find two distinct mechanisms affecting the nanoring deformation at nanorings of different sizes.

Simulation model

In the present study, the temperature elevation process is examined by MD simulations under the canonical ensemble (NVT ensemble). We simulated nanorings of different radii, all constructed of perfect (10,10) armchair SWCNTs bent to form a ring shape. The shape change behavior and the energy of stable structures at different temperatures were calculated. To evaluate the temperature effect, all atoms of the system were assumed to be thermal control atoms at the temperatures simulated. The Nosè–Hoover method is adopted to ensure a constant system temperature throughout the temperature elevation procedure and the Velocity Verlet algorithm (Levesque et al. 1973) is also employed to calculate the trajectories of the atoms. A time step of 0.25 fs was set for the time integration. The REBO II potential was employed to describe short-range bonding

atomic interactions. The total energy of system is thus expressed as

$$E_{ij}^{\mathrm{REBO}} = \sum_{i} \sum_{j(j>i)} [V_{\mathrm{R}}(r_{ij}) - B^{*} V_{\mathrm{A}}(r_{ij})] \quad (1)$$

wherer_{ij} is the distance between atoms i and j. $V_{\mathrm{R}}(r_{ij})$and $V_{\mathrm{A}}(r_{ij})$ are the repulsive and attractive energies between atom i and atom j, respectively. B^{*} is a bond order between atoms i and j. The REBO II potential have expanded database, which leads to a significantly better description of chemical and mechanical properties of hydrocarbon molecules and diamond that compare reasonably well to first-principle prediction. The parameters and detailed introduction of this potential can be found for a SWCNT using concepts developed by Brenner. It has been demonstrated that the cutoff functions of the REBO II potential overestimate the force needed to break a C–C covalent bond. In order to prevent an overestimation of the breaking force of the C–C bond, we use a modified cut-off distance parameter the onset of the covalent interaction cutoff distance from 1.7 to 1.95 Å (Belytschko et al. 2002; Huhtala et al. 2004; Sammalkorpi et al. 2004; Zhang et al. 2005). Therefore, in this present MD simulation, the C–C bond is considered as a so-called breaking bond, where the bond length between the C–C atoms is larger than the cut-off distance of 1.85 Å. In addition, long-range van der Waals interactions are included in the form of a Lennard–Jones potential that is only active at distances greater than the covalent bond lengths. The van der Waals potential energy base on general Lennard–Jones can be written as

$$E_{\mathrm{vdW}}(r) = 4\varepsilon \left[\left(\frac{\sigma}{r}\right)^{12} - \left(\frac{\sigma}{r}\right)^{6} \right] \quad (2)$$

where r is the distance between atoms. For carbon atom the parameter $\varepsilon = 0.0556$ kcal/mol and $\sigma = 3.4$ Å (Battezzatti et al. 1975). Thus, the total potential energy E_{total} is given by

$$E_{\mathrm{total}} = \sum_{i=1}^{N} \sum_{j>i} (E_{ij}^{\mathrm{REBO}} + E_{\mathrm{vdW}}) \quad (3)$$

In order to find the possible minimum-energy structure for nanorings with different radii, we generated the perfect (10,10) armchair type CNT with different initial bond lengths and repeat units (40 atoms, as shown at the inset in Fig. 1), then formed them into closed-ring-like structure by using the coordinate transformation. This structure is clearly not a minimum-energy configuration. There is an excess tension in the inner radius of the ring due to contraction of the C–C bonds, and there is no compensation from the outer radius where extension of the C–C bonds occurs. In order to obtain the equilibrium state of the nanorings of different radii, one hundred thousand time steps were run at 0 K and then the total energy was calculated to find the possible best bond length of C–C required for nanorings composed of 250–450 repeated units with radii differing from 97 to 136 Å. The obtained initial structure was found for those bond lengths with the lowest energies and presented in Fig. 1, which shows total energy for different C–C bond lengths at different units. The possible initial bond lengths of the nanotube necessary to bend into nanoring form are 1.51, 1.51, 1.50, 1.49, 1.48 Å for 250, 300, 350, 400, and 450 units, respectively. The specific corresponding nanoring radii for those unit forms are about 106, 125, 146, 165, and 185 Å, respectively. The thermal stability of five nanorings is investigated by using these initial structures and gradually increasing temperature to 3500 K.

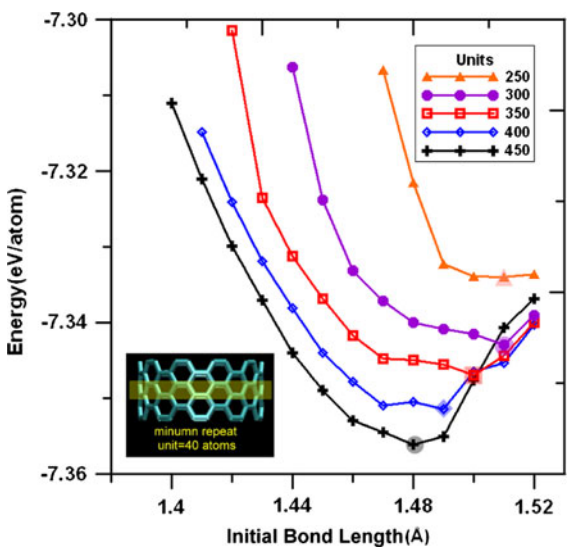

Fig. 1 Total energy of equilibrium state for different initial C–C bond length of nanotubes to fold into nanorings (the values *shadowed* for each different curve are the initial bond length chosen to temperature elevating process)

Results and discussion

Figure 2a shows the final stable structures of five nanorings of different radii after energy minimization by the conjugate-gradient algorithm. For easier comparison, the shapes of these five nanorings made from carbon nanotubes of 250, 300, 350, 400, and 450 repeated units are shown in the same figure with one common origin. The standard deviations of nanoring radii and the average cohesive energies for five nanorings are depicted in Fig. 2b. The samples for the standard deviation are taken from the local radius calculated over 1° intervals from 0° to 360°, a total of 360 samples. The cases of 250 and 300 units show larger values of standard deviations, indicating the equilibrium structures are not close to perfect circular shapes when observed from the top view. Several kinked regions (hereafter "kinks") in the

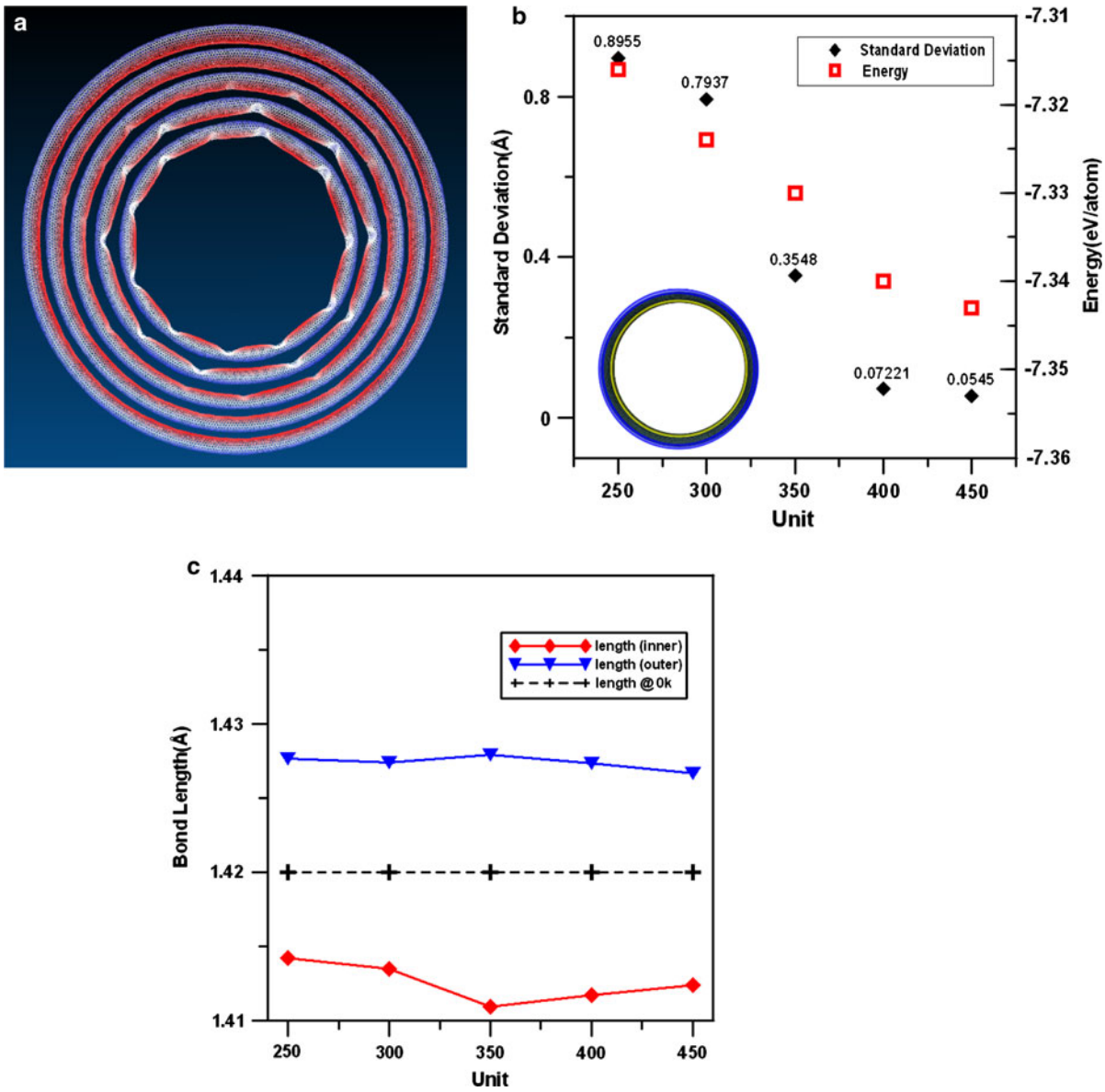

Fig. 2 **a** Morphologies of five nanorings after the energy minimization by the conjugate algorithm; **b** radius standard deviation and average potential energies of the five nanorings; **c** average bond lengths after the energy minimal process at inner and outer walls. The *dashed line* is the stablest bond length of a (10,10) carbon nanotube at 0 K

shape can be clearly seen in Fig. 2a for the cases of 250 and 300 units, resulting in the larger values of standard deviations. The carbon atoms at these kinks are under local distortion relative to their first neighbor atoms. The standard deviations for the other three cases are close to zero, indicating that the shapes of these nanorings are nearly circular in shape. Figure 2c shows the average bond lengths of inner and outer walls of these nanorings, with the most stable bond length of a (10,10) carbon nanotube indicated by the dashed line at 1.42 Å. The outer and inner walls for all nanorings are defined as the outermost and innermost C–C bond chains, colored in yellow and blue, respectively, in the lower left of Fig. 2b. Figure 2c shows the average bond lengths after the energy minimal process at inner and outer walls. The dashed line is the stablest bond length of a (10,10) carbon nanotube at 0 K. It can be seen the average bond lengths of the inner walls are shorter than that of the most stable bond length, while the average bond lengths of the outer walls are longer than the most stable bond length, indicating the inner and outer walls of all nanorings are under conditions of slight compression and tension, respectively. For the cases of 250 and 300 units, the structures have several kinks, which serve to produce average bond lengths of both the inner and outer walls that are closer to the most stable bond length than those of the circle-like nanorings. For the largest three cases, it is clear that both the bond lengths of inner and outer walls approach the bond length of a (10,10) carbon length.

Because the shapes of nanoring structures of different radii are different at 0 K as shown in Fig. 2a, the structural variations during the process of temperature elevation could be very different. Accordingly, the energy difference of an atom between temperatures of T and zero is used to indicate the local structural variation. The formula for the atomic energy difference is defined as follows:

$$\Delta E_i(T) = E_i(T) - E_i(0) \tag{4}$$

where i, $E_i(T)$, and $E_i(0)$ represent atom i of a nanoring, the potential energy of atom i at temperature T, and the referenced potential energy of atom i at temperature 0 K, respectively. Because the variation of potential energy is sensitive both to the distance between two carbon atoms and the angle formed among three neighbor carbon atoms, the value of $\Delta E_i(T)$reflects variance in the structural arrangement of a carbon atom with its first near neighbor carbon atoms at temperature T, relative to its structure at 0 K. A larger value of $\Delta E_i(T)$ for an atom at temperature T indicates a significant local structural variation with change in temperature, while a small value indicates little change in local carbon atom structure relative to its nearest neighbor atoms, even with the change in temperature. It is noted that as usual situation, the significant local structure variation will cause the abrupt change in potential energy. However, in this case, the kinetic energy only changes linearly to the temperature. Thus, the abrupt change will also reflect to the total energy.

Since the inner and outer walls of a nanoring are under compression and tension within the same structure, Figs. 3a, b, 4a, b, 5a, b, 6a, b, to 7a, b display the energy difference plots for the inner and outer walls of nanorings of 250, 300, 350, and 400 units at different temperatures, respectively. The horizontal axes of these figures display different temperatures, and the vertical axes represent the angle around the nanoring from 0°. The largest energy difference value within each 1° interval is plotted in Figs. 3, 4, 5, 6, and 7 and the values are provided in the legends for each figure. In Fig. 3, at temperatures less than 100 K, the nanoring's uniform expansion is indicated by the low color differential at both the inner and outer walls. As the temperature continuously increases, several lines with more contrastive color are apparent, indicating carbon atoms within these portions undergo more significant local distortions relative to their first neighbor atoms, while the carbon atoms within other portions of the nanoring still display relatively uniform thermal expansion, even at high temperatures over 3000 K. It should be noted that the portions undergoing significant local geometric deformations are the portions with local distortion carbon atoms and therefore kinks at the inner wall. The continuous deformations at these portions at higher temperatures are mainly responsible for releasing thermal stresses to remain a stable structure. The energy difference plot for the 300 unit nanoring displays a very similar variation at different temperatures, but the temperature at which several lines with the clear contrasting color begins to appear is higher than that for the nanoring of 250 units. Figure 5 shows the energy difference plot for the 350 unit nanoring which,

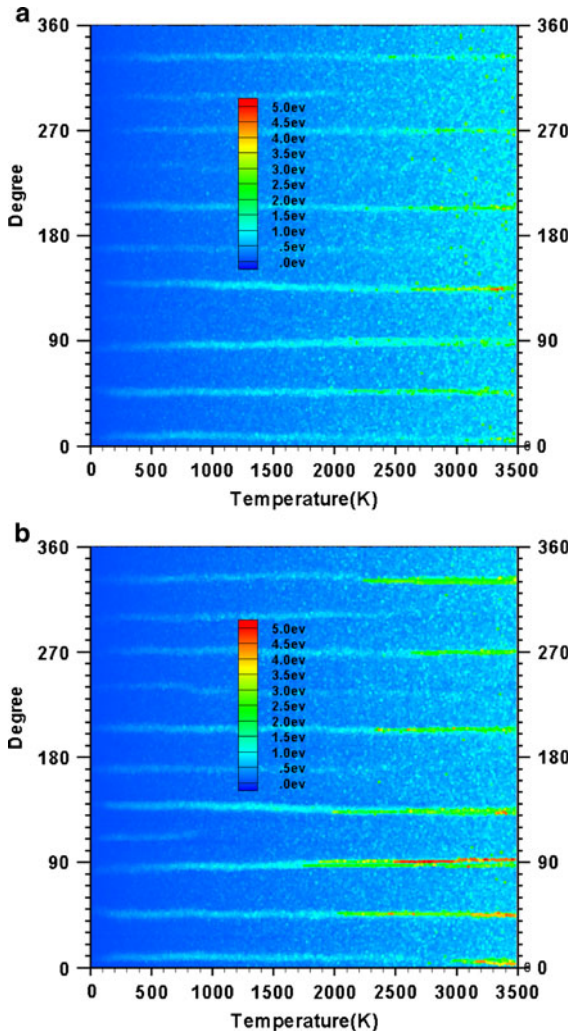

Fig. 3 Distributions of local energy difference of 250 unit nanoring along a temperature gradient at **a** the inner wall; and **b** the outer wall

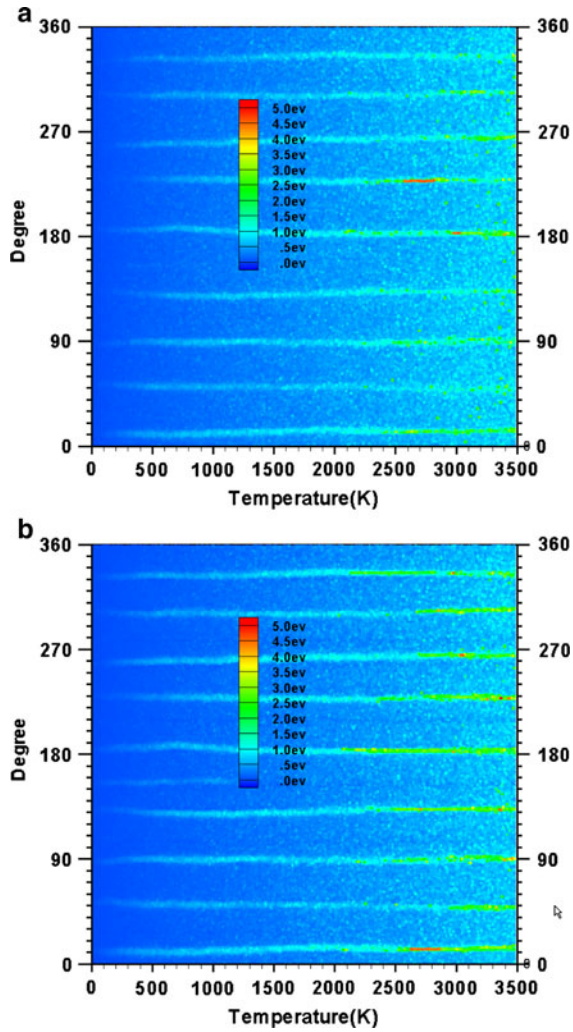

Fig. 4 Distributions of local energy difference of 300 unit nanoring along a temperature gradient at **a** the inner wall; and **b** the outer wall

unlike the 250 or 300 unit ring, has a perfect circle-like shape at 0 K. Uniform expansion can be seen in both the inner and outer walls until the temperature is higher than 500 K, at which point contrasting color lines begin to appear. Although the inner and outer walls of this nanoring are still under compression and tension, the average bond lengths are closer to the equilibrium bond length of a (10,10) CNT. Accordingly, this nanoring maintains its shape at higher temperature better than those with visible kinks at 0 K. Figure 6 demonstrates the energy difference plot of the nanoring of 400 units, and the energy difference variations at different temperatures are notably different from the previous three cases. The outer wall seems to expand almost uniformly as the temperature increases from 0 to 2500 K, with the contrasting lines not appearing until about 2500 K and with the outer wall still maintaining a circular shape even at a high temperature. Even though the outer wall is still under the condition of slight tension, the average bond length is very close to that of a (10,10) CNT. However, since the outer wall remains circular in shape at a higher temperature, the deformation of the inner wall is responsible for releasing thermal stress as the temperature increases from 0 to 2500 K. The energy difference plot of the

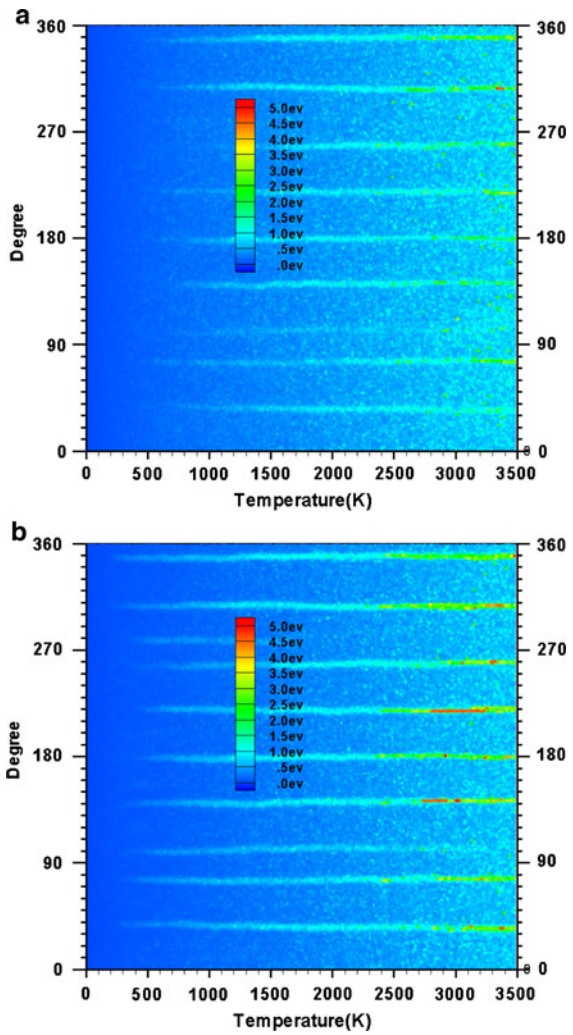

Fig. 5 Distributions of local energy difference of 350 unit nanoring along a temperature gradient at **a** the inner wall; and **b** the outer wall

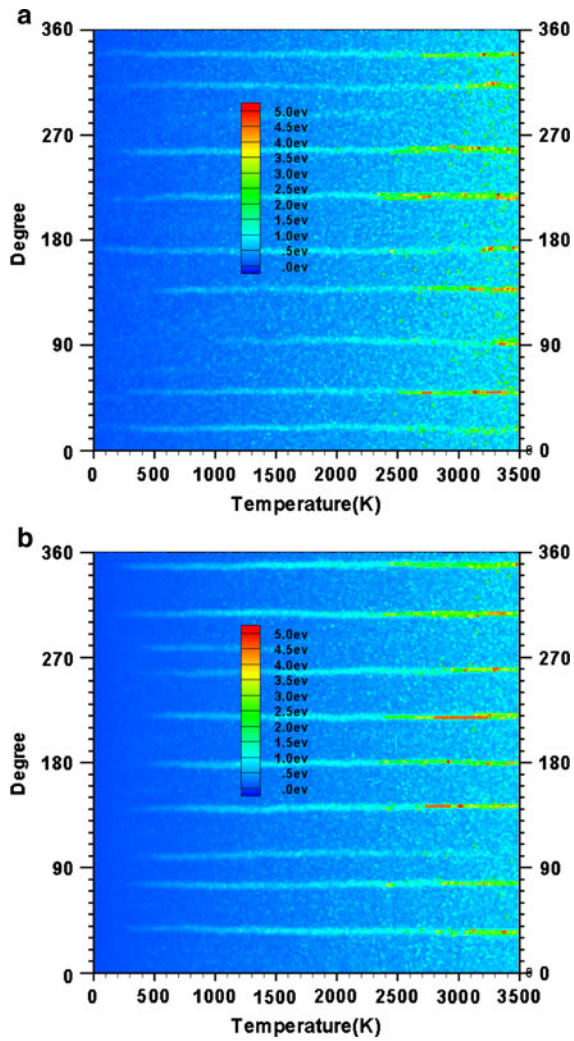

Fig. 6 Distributions of local energy difference of 400 unit nanoring along a temperature gradient at **a** the inner wall; and **b** the outer wall

inner wall shows local deformation at the inner wall begins at about 200 K, even lower than that of the 350 unit case, and only the outer wall undergoes uniform expansion without local distortion. Unlike the 400 unit nanoring, the cases of 250, 300, 350 units display a relationship of deformations between the inner and outer walls in which the local deformations of inner and outer walls occur at roughly the same temperature. For the case of 400 units, Fig. 6 clearly displays an uneven stress condition between inner and outer walls, where even though local distortions occur at several portions of the inner wall from temperatures starting at about 200 K, the outer wall is not influenced by the local distortions of the inner wall until 2500 K. When the temperature is higher than 2500 K, the distortions at the inner wall become so significant that they will induce distortion at the outer wall, as shown in Fig. 6 by the contrasting color lines for the outer wall at about 2500 K. Figure 7 demonstrates the energy difference plot of the nanoring of 450 units, and the energy difference variations at different temperatures are very similar to the case of 400 units. Figure 8 shows the snapshots of different nanorings during the temperature elevating process. The two smallest nanorings have several kinks during the temperature elevation process. However, the biggest nanoring almost maintains its

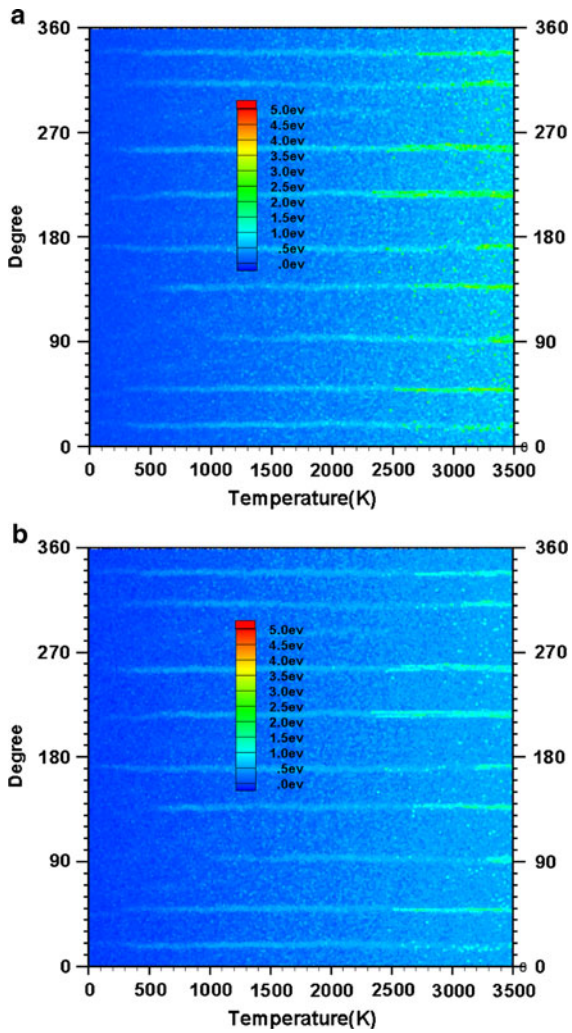

Fig. 7 Distributions of local energy difference of 450 unit nanoring along a temperature gradient at **a** the inner wall; and **b** the outer wall

perfect ring-like form and has no kink during the simulation.

For a closer inspection of the local structural variation, Fig. 9a–f depicts six local top view morphologies of a 400 units nanoring at the same 86–94° segment (of the nanorings' 360°) at temperatures of 1500, 1700, 2000, 2300, 2700, and 2900 K, respectively. At 1500 K, the kink at the inner wall is apparent, and the outer wall at this kink moves slightly in toward the inner wall. From this top view, the width at this kink becomes thinner. At 1700 K, the outer wall at the kink, which slightly moves toward the inner wall at 1500 K, has recovered to a position similar to the other parts of the outer wall, and the kink has shifted more to the left while the width of the nanoring at the kink has become thinner than that at 1500 K. As temperature continuously increases to 2000 K, the position of this kink will remain the same, but will become broader than that at 1700 K. At 2000 K, the width becomes thicker than that at 1700 K and recovers to a width similar to that at 1500 K. At 2300 and 2700 K, the kink will become broader and the width at the kink will become thinner than that at 2000 K. The outer wall at the kink seems more flat and has been influenced by the deformation of the inner wall at these high temperatures. At 2900 K, the width of the nanoring continues to become thinner, but the kink becomes even narrower and sharper than at 2300 and 2700 K. Here, an interesting deformation mechanism of the nanoring of 400 units during the process of temperature elevation has been found. Because the bonding strengths of carbon atoms at the outer wall are very similar to those of a (10,10) CNT, the local deformations of the nanoring to release thermal stress during the process of temperature elevation occurs first at the inner wall. The kink at the inner wall will appear at a specific temperature and the width of the nanoring at the kink will become continuously thinner, to finally influence the outer wall at 1500 K. However, the influenced part of the outer wall will recover to a stable local structure at a higher temperature, which causes the kink to shift. At a higher temperature, since the local deformation at the inner wall cannot cause the deformation of outer wall to release thermal stress, the kink will become broader in order to release the excess thermal stress with the rise in temperature. Finally, at temperatures higher than 2700 K, the width becomes the thinnest and the kink becomes even narrower.

Finally, the comparison of thermal stability between nanorings of different radii is summarized in Fig. 9. The averaged atomic energy difference is used to indicate the thermal stability of nanorings and defined as the following formula:

$$\Delta E(T) = \sum_{i=1}^{N} \Delta E_i(T)/N \tag{5}$$

where $\Delta E_i(T)$ has the same definition in Eq. 4, and N is the total atom number of a nanoring. Consequently, the averaged atomic energy difference is a

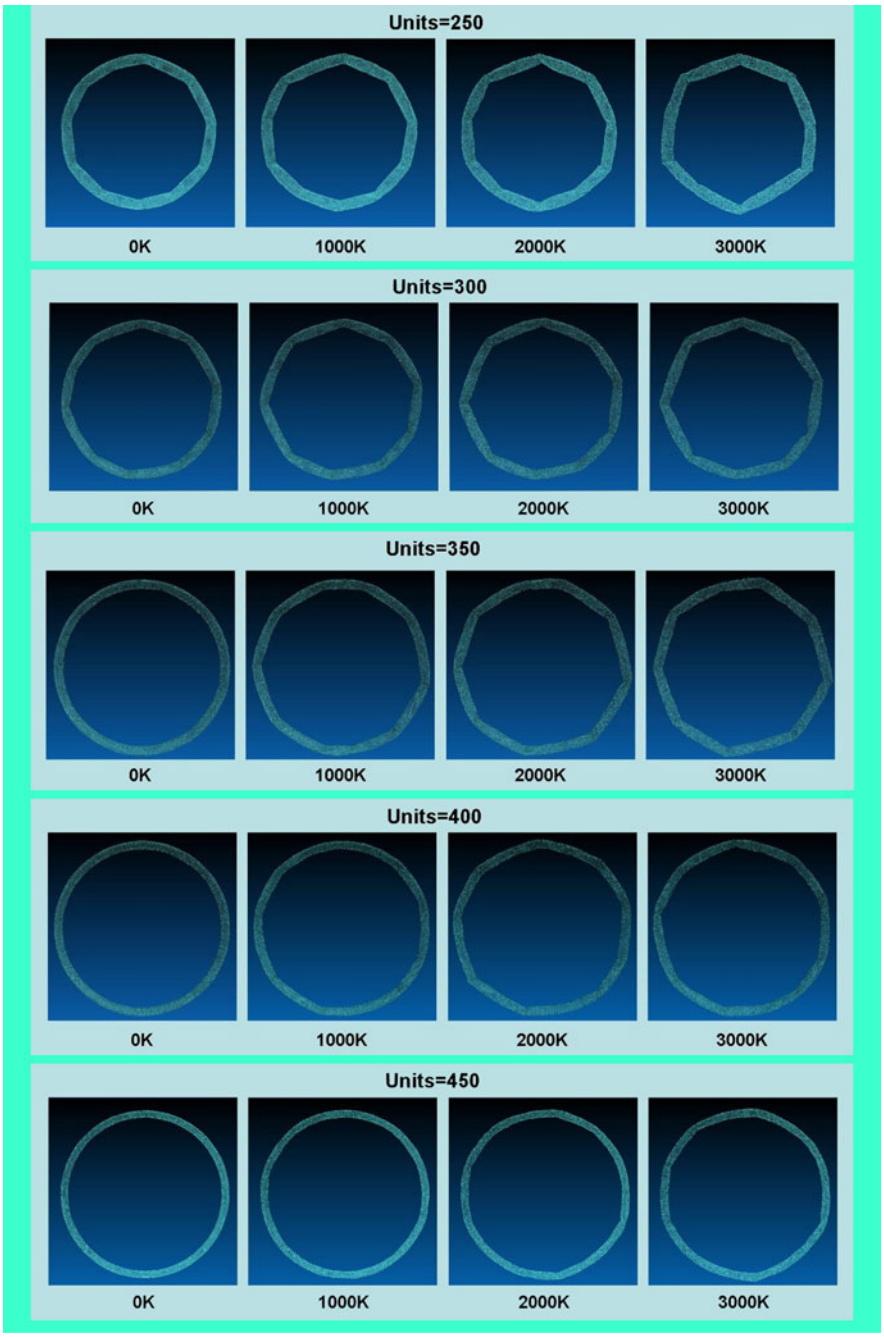

Fig. 8 The snapshots of different nanorings during the temperature elevating process

normalized index to investigate the thermal stability of nanorings of different sizes.

When the temperature elevates from 0 to 500 K, the profiles of the smallest three nanorings display significant variation with the temperature increase, while the other two profiles show values close to zero within this temperature range. For the smallest three nanorings, curvatures are relatively larger, which cause significant local stresses and unstable structures. Once the temperature rises and provides just small amount of kinetic energy, the rearrangements of local atomic structures will take place to release the local stresses and become more stable. Accordingly, the profiles increase with the increase of

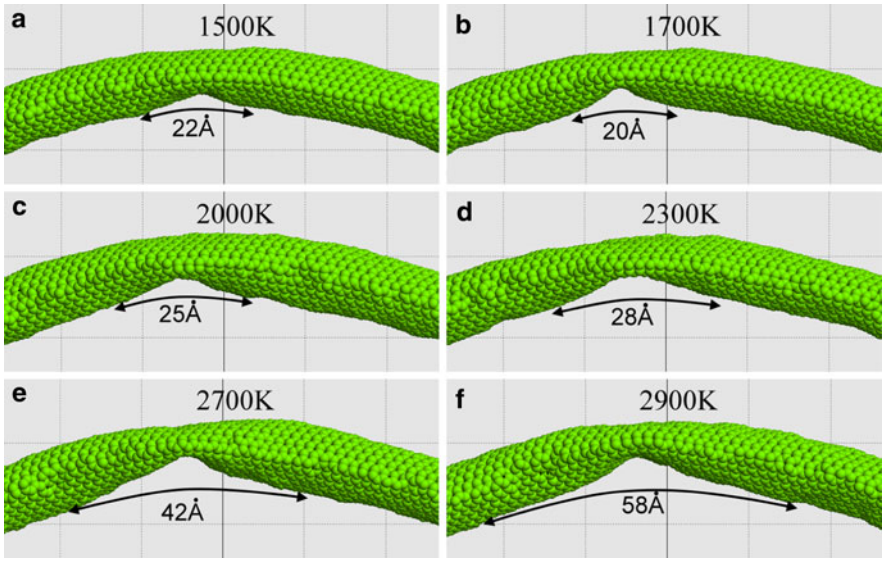

Fig. 9 Morphological variations of a kinked region of an 400 unit nanoring at temperatures of **a** 1500 K, **b** 1700 K, **c** 2000 K, **d** 2300 K, **e** 2700 K, and **f** 2900 K

temperature, and then decreases when the temperature increases. This can be regarded that these nanorings obtain enough kinetic energy to overcome the energy barrier and become relatively stable local minimum structures at about 500 K. For the largest two nanorings, the values of averaged atomic energy difference increases very slowly, indicating there is no significant local structure rearrangement within this temperature range.

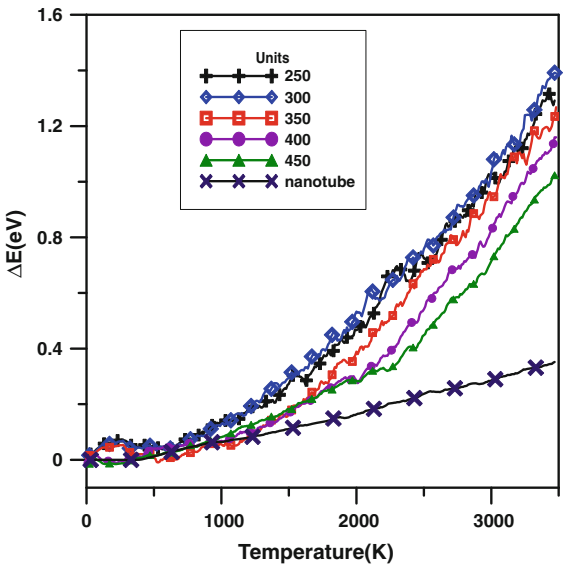

Fig. 10 Profiles of averaged atomic energy difference for five nanorings of different radii

When temperature continuously increases from 500 K, the profiles of the smallest two nanorings monotonically increase with the increase of temperature. However, the slopes of profiles of 350-, 400-, and 450-unit nanorings will become larger after the temperatures are higher than different specific temperatures. The smallest two nanorings undergo significant atomic local rearrangement within a temperature range between 0 and 500 K, so the local structures will not present severe structural change at higher temperatures. For larger nanorings, the local structures undergo slightly and continuously rearrangement within a broader temperature range from 0 K and then display more significant structural rearrangement when the temperatures are over specific values, leading to larger slopes in Fig. 10.

Conclusion

The deformation mechanisms of five nanorings during an increase in temperature have been demonstrated. After energy minimization, the stable structures of the two smallest nanorings display several kinks, and the local deformation for the larger of these two nanorings will occur at a higher temperature than the smaller one. The deformations of inner and outer walls will take place at the same temperature, and remain at higher temperatures. For the

largest three cases, the morphologies of nanorings from the top view display circular shapes at 0 K. For the case of 350 units, with a nanoring radius of 146 Å, the thermal deformation process is very similar to the smallest two cases, but the temperature at which the thermal deformation begins is higher. For the cases of 400 and 450 units, with nanoring radii of 165 and 185 Å, thermal deformation will first take place at the inner wall of the nanoring, and then the deformation at the inner wall will finally induce the deformation of the outer wall at a higher temperature. Although the structures of all nanorings are under both slight compression and slight tension at the inner and outer walls, respectively, the local structures with an average bond length close to that of a (10,10) CNT can maintain their shape at a higher temperature.

Acknowledgments The authors would like to thank the National Center for Theoretical Sciences and National Science Council of Taiwan for supporting this study, under Grant Nos. NSC95-2221-E-159-003-MY3 and NSC97-2221-E-492-003-MY2.

References

Battezzatti BY, Pisani C, Ricca F (1975) Equilibrium conformation and surface motion of hydrocarbon molecules physisorbed on graphite. J Chem Soc Faraday Trans II 71:1629–1639

Belytschko T, Xiao SP, Schatz GC, Ruoff RS (2002) Atomistic simulations of nanotube fracture. Phys Rev B 65:235430

Berber S, Kwon YK, Tomanek D (2003) Bonding and energy dissipation in a nanohook assembly. Phys Rev Lett 91:165503

Brenner DW (1990a) Atomistic computer simulations of the reactive dynamics of diamond surfaces. Carbon 28:769–770

Brenner DW (1990b) Empirical potential for hydrocarbons for use in simulating the chemical vapor deposition of diamond films. Phys Rev B 42:9458–9471

Brenner DW, Shenderova OA, Harrison JA, Stuart SJ, Ni B, Sinnott SB (2002) A second-generation reactive empirical bond order (rebo) potential energy expression for hydrocarbons. J Phys Condens Matter 14:783–802

Chen N, Lusk MT, van Duin ACT, Goddard WA (2005) Mechanical properties of connected carbon nanorings via molecular dynamics simulation. Phys Rev B 72:085416

Dunlap BI (1992) Connecting carbon tubules. Phys Rev B 46:1933

Hod O, Rabani E (2003) Carbon nanotube closed-ring structures. Phys Rev B 67:195408

Hoover WG (1985) Canonical dynamics: equilibrium phase-space distributions. Phys Rev A 31:1695–1697

Huhtala M, Kuronen A, Kaski K (2002a) Carbon nanotube structures: molecular dynamics simulation at realistic limit. Comput Phys Commun 146:30–37

Huhtala M, Kuronen A, Kaski K (2002b) Computational studies of carbon nanotube structures. Comput Phys Commun 147:91–96

Huhtala M, Krasheninnikov AV, Aittoniemi J, Stuart SJ, Nordlund K, Kaski K (2004) Mechanical properties of carbon nanotubes with vacancies and related defects. Phys Rev B 70:245416

Kwon YK, Berber S, Tomanek D (2004) Thermal contraction of carbon fullerenes and nanotubes. Phys Rev Lett 92:015901

Latge A, Rocha CG, Wanderley LAL, Pacheco M, Orellana P, Barticevic Z (2003) Defects and external field effects on the electronic properties of a carbon nanotube torus. Phys Rev B 67:155413

Latil S, Roche S, Rubio A (2003) Persistent currents in carbon nanotube based rings. Phys Rev B 67:165420

Levesque D, Verlet L, Kurkijar J (1973) Computer experiments on classical fluids. IV. Transport properties and time-correlation functions of the Lennard–Jones liquid near its triple point. Phys Rev A 7:1690–1700

Lin MF (1998a) Low-frequency optical excitations in zigzag carbon tori. Phys Rev B 58:3629–3632

Lin MF (1998b) Magnetooptical properties of carbon toroids. J Phys Soc Jpn 67:2218–2221

Lin MF (1998c) Transport properties of carbon toroids. J Phys Soc Jpn 68:3744–3745

Lin MF, Chuu DS (1998a) Electronic states of toroidal carbon nanotubes. J Phys Soc Jpn 67:259–263

Lin MF, Chuu DS (1998b) Persistent currents in toroidal carbon nanotubes. Phys Rev B 57:6731

Liu J, Dai HJ, Hafner JH, Colbert DT, Smalley RE, Tans SJ, Dekker C (1997) Fullerene 'crop circles'. Nature 385:780–781

Liu L, Jayanthi CS, Wu SY (2001) Structural and electronic properties of a carbon nanotorus: effects of delocalized and localized deformations. Phys Rev B 64:033412

Liu L, Guo GY, Jayanthi CS, Wu SY (2002) Colossal paramagnetic moments in metallic carbon nanotori. Phys Rev Lett 88:217206

Liu P, Zhang YW, Lu C (2005) Atomistic simulations of formation and stability of carbon nanorings. Phys Rev B 72:115408

Oh DH, Park JM, Kim KS (2000) Structures and electronic properties of small carbon nanotube tori. Phys Rev B 67:1600

Pozrikidis C (2008) Structure of carbon nanorings. Comput Mater Sci 43:943–950

Sammalkorpi M, Krasheninnikov A, Kuronen A, Nordlund K, Kaski K (2004) Improved mechanical load transfer between shells of multiwalled carbon nanotubes. Phys Rev B 70:045404

Shea HR, Martel R, Avouris P (2000) Electrical transport in rings of single-wall nanotubes: one-dimensional localization. Phys Rev Lett 84:4441–4444

Shyu FL, Tsai CC, Chang CP, Chen RB, Lin MF (2004) Magnetoelectronic states of carbon toroids. Carbon 42:2879–2885

Tsai CC, Shyu FL, Chiu CW, Chang CP, Chen RB, Lin MF (2004) Magnetization of armchair carbon tori. Phys Rev B 70:075411

Zhang SL, Mielke SL, Khare R, Troya D, Ruoff RS, Schatz GC, Belytschko T (2005) Mechanics of defects in carbon nanotubes: atomistic and multiscale simulations. Phys Rev B 71:115403

Zhu SQ, Wang X (2007) Effect of environmental temperatures on elastic properties of single-walled carbon nanotube. J Therm Stress 30:1195–1210